A UTD/FDTD Investigation on Procedures to Assess Compliance of Cellular Base-Station Antennas With Human-Exposure Limits in a Realistic Urban Environment

Paolo Bernardi, *Life Fellow, IEEE*, Marta Cavagnaro, *Member, IEEE*, Renato Cicchetti, *Senior Member, IEEE*, Stefano Pisa, *Member, IEEE*, Emanuele Piuzzi, and Orlandino Testa

***Abstract*—In this paper, different exposure situations for a subject standing inside a room of a building with a window facing a rooftop-mounted base-station antenna are analyzed. The study is accomplished by using a technique combining the uniform asymptotic theory of diffraction and the finite-difference time-domain method, suitable to characterize human exposure in realistic urban environments at a reasonable computational cost. The different exposure conditions examined are analyzed to highlight the problems related to compliance assessment procedures in complex exposure scenarios and to suggest some possible solutions. A comparison of the results obtained in these scenarios with those computed neglecting the presence of the room walls (free-space situations) evidences that, under certain conditions, average exposure field levels and specific absorption rates (SARs) in the realistic environments can be higher than in free space, thus demonstrating that compliance assessment carried out in free space can yield nonconservative results. As concerns implications of field nonuniformities, typical of realistic urban environments, on SAR values, the results show that the whole-body averaged SAR is related to the average field value, provided the averaging procedure is appropriately chosen to cover all the volume occupied by the subject (V_S) and not only a vertical surface. Local SAR values, instead, show a more complex relation with the exposure field, such that considering only the V_S-averaged field value for compliance assessment might lead to an underestimation of the real exposure level, while using the peak of the field in V_S leads to a remarkable overestimation.**

***Index Terms*—Beam tracing, compliance assessment, dosimetry, finite-difference time-domain (FDTD) methods, human exposure, land mobile radio cellular systems, uniform theory of diffraction (UTD).**

I. Introduction

THE STEADY increase in the number of subscribers of mobile telecommunication systems is pushing toward an enhancement of the capacity of the systems themselves. As a result, more and more base stations are being installed on the rooftop of existing buildings in densely populated areas. These installations are giving rise to widespread concerns among the population about possible detrimental effects to human health deriving from exposure to the electromagnetic fields radiated by base-station antennas. Therefore, the problem of defining reliable compliance assessment procedures for base-station installations in urban areas is a very timely one.

The currently adopted procedures for the assessment of base-station safety, with respect to human exposure, are mainly based on a comparison of the exposure field value with reference levels suggested by exposure guidelines [1]–[4]. This is due to the great difficulty in carrying out an on-site dosimetric evaluation of specific absorption rate (SAR) inside the exposed subject, necessary for a direct comparison with basic restrictions. However, reference levels have been derived from basic restrictions under the assumption of uniform plane-wave exposure and, hence, their validity is demonstrated only under this particular condition. On the other hand, the exposure field in an urban environment is far from being uniform due to the presence of many reflection and diffraction processes and, therefore, the problem arises of which field value should be compared with the reference one. This has resulted in different regulatory bodies issuing different compliance assessment procedures that, under some aspects, do not agree one with the other.

The IEEE exposure guidelines [1], which are largely at the base of Federal Communications Commission (FCC) regulations [2], state that, in the case of nonuniform exposure conditions, the field should be averaged on a vertical surface equivalent to the projected human body area, and that the use of the exposure field peak value, instead of the average one, seems to be unnecessarily conservative. The International Commission on Non-Ionizing Radiation Protection (ICNIRP) guidelines [3], which have been adopted by the European Communities (EC) to issue a European Recommendation [4], state that when the exposure is nonuniform, the field should be averaged on a vertical surface equivalent to the projected human body area, but only to establish whole-body averaged SAR compliance. No correlation, instead, is given between the local SAR and exposure field and, therefore, local SAR compliance must be directly assessed through a dosimetric analysis. A compliance procedure, based on the EC Recommendation, has been recently issued by the European Committee for Electrotechnical Standardization (CENELEC) [5]. This procedure, in order to overcome the necessity of performing a complete dosimetric assessment, allows local SAR compliance evaluation through

Manuscript received April 17, 2003.
The authors are with the Department of Electronic Engineering, “La Sapienza” University of Rome, 00184 Rome, Italy (e-mail: bernardi@die.uniroma1.it).
Digital Object Identifier 10.1109/TMTT.2003.819773

a comparison of the peak value of the exposure field with the corresponding reference level (conservative approach). Finally, other procedures for base-station compliance assessment, like those issued by the Italian Electrotechnical Committee (CEI) [6] suggest that, if compliance is evaluated through a numerical approach rather than measurements, the numerical analysis can be performed neglecting the presence of the environment (free-space condition), thus eliminating the problem of field nonuniformities. The rationale at the basis of such procedure is that free space should represent a conservative exposure situation.

Due to the many contrasting approaches to base-station compliance assessment above presented, an accurate dosimetric analysis performed under realistic urban-scenario exposure conditions seems necessary to highlight the basic requirements that a compliance assessment procedure should have.

Up to now, only a few works are available in the literature concerning human exposure to base-station antennas [7]–[16]. In [7] and [8], attention was focused on the determination of simplified and efficient numerical and analytical models to evaluate field levels near a base-station antenna, but no dosimetric analysis was performed. In [9], the accuracy of finite-difference time-domain (FDTD) models for the evaluation of the near field of base-station antennas was investigated through a comparison with measurements. Finally, in [10], a spherical-wave expansion technique was proposed to evaluate the near field starting from measurements performed on a spherical surface surrounding the antenna. Other papers have dealt with the evaluation of induced SAR in an exposed subject. In [11] and [12], the feasibility of mixed experimental/numerical procedures to compute the induced SAR beginning from measured exposure field distributions was studied, but the relation between the SAR and impinging field values was not investigated. A thorough numerical and experimental dosimetric analysis was performed in [13], where only exposure of a subject in close proximity of the antenna in a free-space environment was considered. A similar numerical analysis for a wide range of distances in front of the antenna was performed in [14]. More complex exposure situations were analyzed in [15], where the numerical technique employed allowed representation of corner-reflector-like urban scenarios. Finally, a more sophisticated technique was presented in [16], but it was only applied to the study of a single exposure condition for a microcell site.

In this paper, some exposure situations in realistic urban scenarios, comprising an indoor environment in which the field penetrates propagating through the room walls and glass window, will be analyzed. The study will be accomplished by using a hybrid uniform asymptotic theory of diffraction/finite-difference time-domain (UTD/FDTD) method, suitable to analyze human exposure in realistic urban environments at a reasonable computational cost. Both the global system for mobile communications (GSM) and the universal mobile telecommunications system (UMTS) frequency bands will be considered. The different exposure conditions examined will be analyzed to highlight some key points related to compliance assessment procedures.

II. Methods and Models

The FDTD method is currently the most used technique in electromagnetic dosimetry problems. In fact, it allows an accurate simulation of the field source (antenna) and a detailed modeling of nonhomogeneous scatterers having arbitrary shape (human body) [17]–[19]. This method, however, is not efficient to study scattering problems involving large regions (urban environment) due to huge memory and CPU time requirements. In order to overcome this problem, in this paper, the FDTD method is used in conjunction with a UTD model, suitable to characterize very efficiently the field propagation in complex large environments.

As a first step, a high-frequency UTD model is used to evaluate the incident field on the exposed subject. Such model employs the heuristic diffraction coefficient proposed in [20] to accurately model the field scattered from penetrable objects. Higher-order geometrical-optics (GO) reflections and transmissions (up to five) are computed, while only first-order diffraction phenomena are considered [21]. The elements forming the environment are modeled as junctions of thin flat multistrate lossy/lossless plates of different materials [20], and the characteristics of the transmitting antenna are taken into account by means of its radiation pattern. In the numerical implementation of the UTD model, a beam-tracing (BT) algorithm [21], [22] has been adopted to derive the electromagnetic ray paths starting from the base-station antenna.

As a second step, the exposure field obtained with the UTD model is employed to derive equivalent surface currents, which, making use of the equivalence principle, are used to excite the field in the FDTD region where the exposed subject is located [15], [23]. The FDTD domain is closed applying a five-cell uniaxial perfectly matched layer (UPML) absorbing boundary condition with a linear profile and 1% reflection coefficient [24].

It must be observed that, while the FDTD method is a technique that operates in the time domain, the UTD model works in the frequency domain. This means that, in the FDTD algorithm, the UTD-derived equivalent currents are immediately set to their time–harmonic steady-state value. On the other hand, the FDTD method requires the setting of initial conditions, namely, the values of the electromagnetic field inside the FDTD at the initial time step, which are commonly set to zero. This mismatch results in the injection of electric and magnetic charges on the Huygen's equivalence surface during the early transient. As a consequence, the final steady-state field distribution is affected by a dc offset that has been eliminated by applying a discrete Fourier transform (DFT), at the frequency of interest, to the electromagnetic fields computed in the time domain.

III. Results and Discussion

A. Description of the Realistic Exposure Scenarios

The above-described UTD/FDTD technique is used to analyze two typical exposure situations (the "Front" case and "Oblique" case) in an urban scenario, as depicted in Fig. 1.

In both situations, a panel antenna is mounted on the rooftop of a building on top of a 3-m-high mast, with 6° mechanical down-tilting. For each situation, both the case of a GSM 900

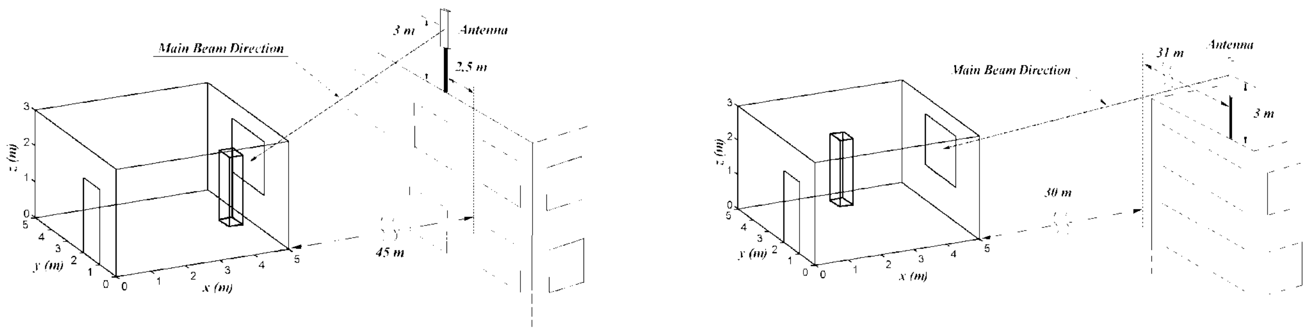

(a) (b)

Fig. 1. Considered urban scenarios. (a) "Front" case. (b) "Oblique" case. The region where the subject is located is evidenced by the parallelepiped box. The room wall at $x = 5$ m is the external wall.

and UMTS antenna are considered in order to analyze the differences between the frequencies employed by the two communication systems. In particular, for GSM 900, the antenna is supposed to operate at 947.5 MHz, while for UMTS, the considered frequency is 2140 MHz (both frequencies fall in the middle of the base-station transmit band for the respective communication systems [25], [26]). In all cases, the antenna is supposed to radiate a power of 30 W. This power level represents a typical value for a four-transmitter GSM 900 base-station operating in an urban environment, and the same value is also used here for UMTS even though, in this case, radiated power levels are expected to be somewhat lower. Indeed, for the purposes of this study, which mainly investigates the relationship between the SAR and exposure field, the radiated power does not play an important role. The considered base-station antenna for GSM 900 is a Kathrein 730-691 panel antenna, constituted by six parallel pairs of vertical half-wavelength dipoles, aligned on a vertical axis. The antenna presents a metallic flat reflector at the back of dimensions 25 cm $\times$ 200 cm [9]. The corresponding three-dimensional radiation pattern has been obtained through the Method of Moments (MoM) employing the freely available NEC code [27]. The obtained -3-dB apertures on the horizontal and vertical planes are approximately 64° and 8°, respectively, while the antenna gain is 18 dBi. These data, derived from MoM simulations, are in good agreement with the antenna characteristics given by the manufacturer. The same radiation pattern is also employed for the UMTS antenna because of the similar radiating characteristics of base-station antennas currently on the market for the two considered systems.

In the "Front" case, a second building, having the same height of the first one, is placed just in front of the base-station antenna, on the opposite side of a 45-m-wide metropolitan avenue, and a subject is supposed to stand, on the last floor of this building, behind a 2 m $\times$ 1.5 m glass window, as evidenced by the parallelepiped box in Fig. 1(a). The window is placed in the direction of the antenna main beam. In the "Oblique" case, instead, a second building, still having the same height, is on the opposite side of a 30-m-wide avenue, and a subject is supposed to stand in a room on the last floor (as in the "Front" case), but near a room wall, as evidenced by the box in Fig. 1(b). The room window "sees" the antenna under an angle of approximately 45° and, as in the previous case, is placed in the direction of the main beam of the base-station antenna. The distance between the glass window and antenna is approximately the same both for the "Front" and "Oblique" cases (45 m). The geometrical and electrical characteristics of the materials forming the environment are reported in Table I [28].

TABLE I
CHARACTERISTICS OF THE MATERIALS FORMING THE ENVIRONMENT

Material	Thickness (cm)	947.5 MHz		2140 MHz	
		ε_r	σ (S/m)	ε_r	σ (S/m)
Ceiling and floor	25.0	10.0	0.060	7.9	0.089
External brick wall	22.0	5.1	0.010	5.2	0.028
Internal brick wall	12.0	5.1	0.010	5.2	0.028
Wooden door	4.0	3.0	0	3.0	0
Glass window	0.5	3.0	0	3.0	0

For each realistic exposure condition, a corresponding free-space situation, obtained maintaining the antenna and subject in the same positions and removing the buildings, is also considered.

The nonhomogeneous phantom used to model the exposed subject has a 3-mm resolution and has been obtained from a tissue-classified version of the "Visible Human Project" data set developed at Brooks Air Force Base Laboratories, Brooks AFB, TX [29]. The chosen 3-mm cell dimension corresponds to less than one-tenth and one-fifth of the wavelength in the tissue with the highest permittivity in the GSM 900 and UMTS frequency bands, respectively. This choice guarantees a good accuracy for the FDTD simulations thanks to the highly lossy nature of the biological tissues [30], [31]. The body model has a total height of 180 cm and 31 different types of tissues/organs have been evidenced. For the electrical characterization of the tissues at the two frequencies of interest, the data reported in [32] and [33] have been used.

B. Exposure Field and SAR Values

A validation case of the UTD/FDTD technique can be found in [34], where the necessity of such a technique for an accurate assessment of human exposure in a realistic urban scenario has been also demonstrated. In this paper, the technique is directly applied to study the exposure situations corresponding

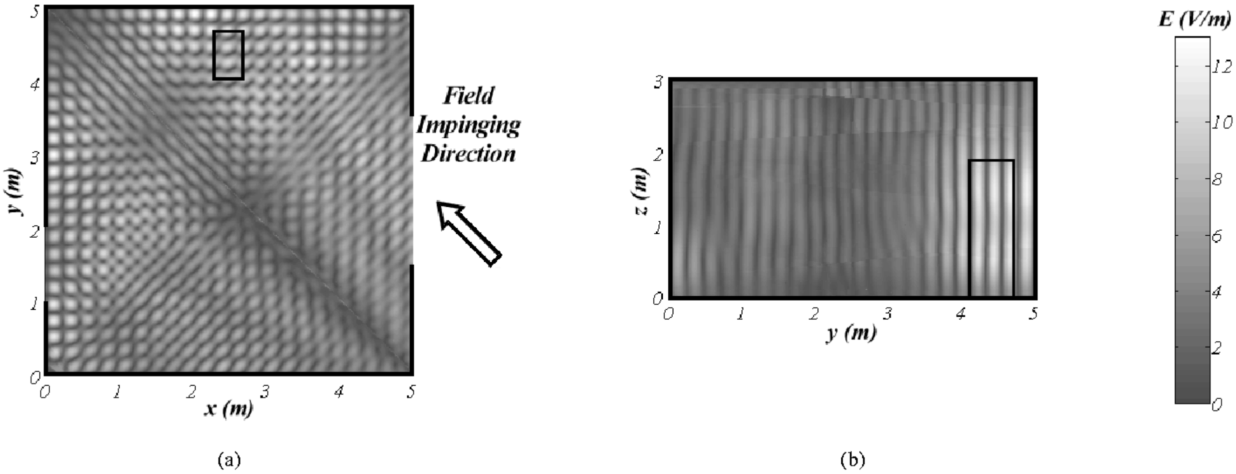

Fig. 2. Field distributions (rms values) inside the empty room for the "Oblique" GSM case. (a) Horizontal plane at $z = 1$ m. (b) Vertical section at $x = 2.50$ m. The region where the subject will be placed is marked by the rectangle. The presence of the walls and openings (glass window, wooden door) is also evidenced.

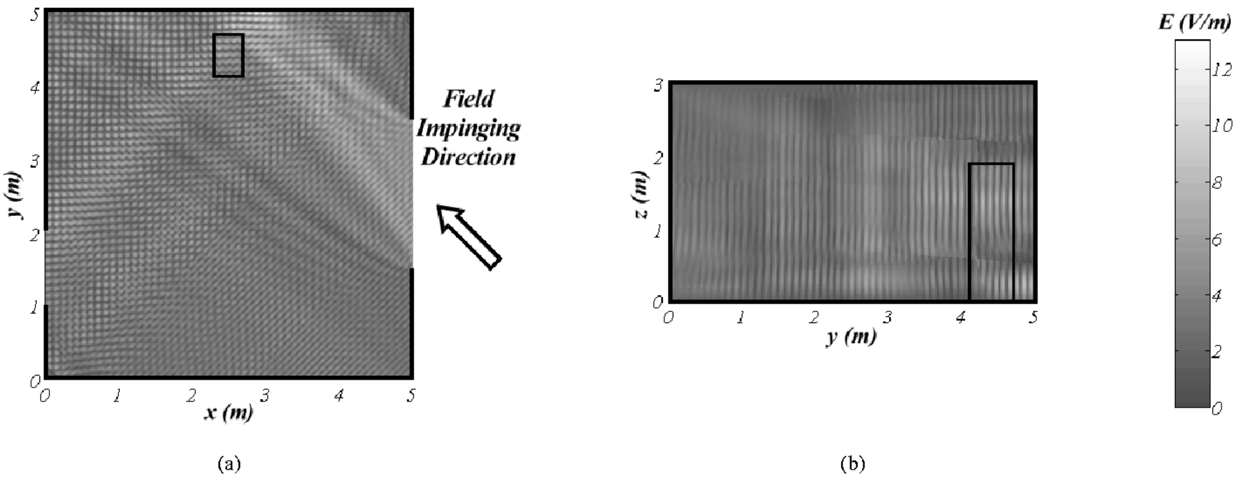

Fig. 3. Field distributions (rms values) inside the empty room for the "Oblique" UMTS case. (a) Horizontal plane at $z = 1$ m. (b) Vertical section at $x = 2.50$ m. The region where the subject will be placed is marked by the rectangle. The presence of the walls and openings (glass window, wooden door) is also evidenced.

to the "Front" and "Oblique" cases and the related free-space situations.

For both the "Front" and "Oblique" case, and for the two considered frequencies, the field distribution inside the empty room is analyzed before studying the subject exposure. As an example, the rms field maps predicted for the "Oblique" cases by means of the UTD model inside the room on a horizontal plane at a height of 1 m above the floor and on a vertical section at $x = 2.50$ m are reported for the GSM case in Fig. 2(a) and (b), respectively. Similarly, Fig. 3 shows the rms field maps on the same planes for the UMTS case. The maps show the complex field distribution due to the multiple reflection and diffraction processes caused by the edges and junctions between the different materials (brick walls, glass window, and wooden door) forming the environment. The region where the subject will be placed, evidenced by the rectangle, is the one with the highest field levels. This region has total dimensions of 34.2 $\times$ 58.8 $\times$ 187.8 cm^3, centered at $x = 4.50$ m, $y = 2.50$ m, $z = 94.7$ cm for the "Front" case, and $x = 2.50$ m, $y = 4.38$ m, and $z = 94.7$ cm for the "Oblique" case. The UTD computations necessary to obtain the above-reported numerical results require a simulation time of approximately 3 h on a workstation equipped with a 2.0-GHz Xeon processor.

The exposure field values (in the absence of the subject) obtained for the different scenarios under consideration are reported in Table II. The acronyms "GSM" and "UMTS" in the "Exposure Situation" column denote the kind of system considered, while "Room" and "FS" denote the realistic exposure condition and equivalent free-space situation, respectively. The first two columns of Table II show the peak $(E_{\text{vol peak}})$ and average $(E_{\text{vol ave}})$ rms exposure field values over the entire parallelepiped volume where the subject will be placed. The slight difference between maximum and average exposure field values in the free-space situations evidences that the field is almost uniform because the parallelepiped volume is entirely within the antenna main beam. The last two columns of Table II, instead, report the peak $(E_{\text{sup peak}})$ and average $(E_{\text{sup ave}})$ rms exposure field values over a vertical yz-section of the parallelepiped volume (as requested by exposure guidelines [1]–[4]). However, rather than a single value, the minimum $(\min)$ and max-

TABLE II
EXPOSURE FIELD rms VALUES (IN THE ABSENCE OF THE SUBJECT) FOR THE DIFFERENT SCENARIOS—$E_{\mathrm{vol\ peak}}$ AND $E_{\mathrm{vol\ ave}}$ ARE THE PEAK AND AVERAGE rms EXPOSURE FIELD VALUES OVER THE ENTIRE PARALLELEPIPED VOLUME WHERE THE SUBJECT IS LOCATED—$E_{\mathrm{sup\ peak}}$ AND $E_{\mathrm{sup\ ave}}$ ARE THE PEAK AND AVERAGE rms EXPOSURE FIELD VALUES OVER A VERTICAL YZ-SECTION OF THE VOLUME (min AND max DENOTE THE MINIMUM AND MAXIMUM VALUES OBTAINED MOVING THE SECTION INSIDE THE VOLUME ALONG THE x-AXIS)

Exposure Situation	$E_{vol\ peak}$ (V/m)	$E_{vol\ ave}$ (V/m)	$E_{sup\ peak}$ (V/m)		$E_{sup\ ave}$ (V/m)	
			min	*max*	*min*	*max*
Front GSM FS	5.26	5.16	5.21	5.26	5.14	5.18
Front GSM Room	7.85	4.61	4.17	7.85	2.91	5.80
Oblique GSM FS	4.99	4.90	4.96	4.99	4.89	4.91
Oblique GSM Room	12.26	5.85	7.76	12.26	4.61	7.31
Front UMTS FS	5.28	5.16	5.21	5.28	5.15	5.18
Front UMTS Room	7.48	4.44	4.81	7.48	3.33	5.37
Oblique UMTS FS	5.01	4.90	4.98	5.01	4.89	4.91
Oblique UMTS Room	10.95	3.96	7.38	10.95	3.62	4.38

imum (max) field values are reported because both the peak and average depend on where exactly the surface is placed. This is better evidenced by Fig. 4(a) and (b), which shows, for the "Front" case, for GSM and UMTS base stations, respectively, the peak and average field values as a function of the position of the vertical surface inside the region where the subject will be placed.

After studying the empty room, exposure of the human subject is considered. The FDTD computations, necessary to evaluate the SAR values, require a simulation time of approximately 6 h to reach steady state with a memory occupation of 1.5 GB on the same workstation employed for the UTD computations. The computed SAR values for all the studied scenarios are reported in Table III. More detailed, as requested by the most recognized exposure guidelines [1]–[4], the considered SAR values are: 1) whole-body averaged SAR ($\mathrm{SAR_{WB}}$) [1]–[4]; 2) peak 1-g averaged SAR over the body, except hands, wrists, feet, and ankles ($\mathrm{SAR_{1\ g}}$) [1], [2]; 3) peak 10-g averaged SAR over the head and trunk ($\mathrm{SAR_{10\ g}}$) [3], [4]; and 4) peak 10-g averaged SAR over the extremities ($\mathrm{SAR_{10\ g\ extr}}$) [1]–[4]. In the case of peak values, an indication of the body part where these values have been obtained is also reported. The algorithm adopted for $\mathrm{SAR_{1\ g}}$ and $\mathrm{SAR_{10\ g}}$ computation uses a cubic volume built adding the FDTD-grid cells around the investigation point. This cubic volume is progressively expanded until the first cube exceeding the desired mass is obtained. At this point, the total power absorbed in the desired mass is evaluated through a linear interpolation between the total power absorbed in this last cube and in the previous one. The SAR is then computed dividing this power by the desired mass. Only cubes with an air-cell inclusion ratio not exceeding 10% of the total volume are considered.

It must be noted that, in all cases, the $\mathrm{SAR_{10\ g\ extr}}$ is obtained in the hands or feet and, therefore, a unique value can be used both for standards limiting extremities to hands, wrists, feet, and ankles [1], [2] and for standards identifying extremities with all limbs [3], [4]. The only exception is the "Front UMTS FS" situation, in which the reported $\mathrm{SAR_{10\ g\ extr}}$ value is obtained in the elbow and, therefore, is relevant only for the second group of standards. For the first one, the relevant $\mathrm{SAR_{10\ g\ extr}}$ value, obtained in the hands, is 4.41 mW/kg.

Analysis of Tables II and III immediately evidences that equivalent free-space conditions do not always represent a conservative scenario. This is clearly shown by the "Oblique" case, where, for GSM base station, the volume-averaged field value is increased by 20% when the presence of the building is considered (see Table II), and the peak SARs show up to a twofold increase, as compared to the corresponding free-space situation (see Table III). The increase of the volume-averaged field value in the considered environment with respect to the free-space one is caused by the field-confining effect, which takes place in an indoor environment due to the multiple field reflection and diffraction phenomena. This particular result represents an evidence against the use of simplified exposure conditions when assessing base-station compliance through a numerical approach.

Still looking at Table III, a comparison between GSM 900 and UMTS frequencies shows that, under free-space conditions, $\mathrm{SAR_{WB}}$ decreases in the highest frequency band due to the smaller penetration depth of the field, while peak SARs increase due to the higher losses in the external tissue layers. However, when a realistic environment is considered, the above-discussed behavior can be altered by the different reflection and diffraction phenomena occurring at the two frequencies. This is clearly evidenced by the "Oblique" case, where $\mathrm{SAR_{1\ g}}$ decreases from 10.67 to 4.90 mW/kg as the frequency increases.

C. Relation Between Exposure Field and SAR Values

The most relevant open problem in current compliance assessment procedures is the relation existing between local SAR and exposure field values, and the consequent choice of comparing the average [1] or maximum [5] field level with the reference one. A comparison between the realistic exposure scenarios and the corresponding free-space situations can help to derive such a field–SAR relation.

To this end, Table IV reports, for each environment, the squared ratios (because of the quadratic relation between the SAR and electric field) between the different field values and the almost constant value computed in the related free-space condition (5.2 V/m in the "Front" cases and 4.9 V/m in the "Oblique" cases). Table V, instead, reports the ratios between SAR values in the considered scenario and the corresponding ones in free-space conditions.

A comparison of Tables IV and V allows to draw the following conclusions.

- $\mathrm{SAR_{WB}}$ values are well correlated to the volume-averaged exposure field value $E_{\mathrm{vol\ ave}}$. This is evidenced in Table VI, which reports, for each considered environment, the relative error made assessing $\mathrm{SAR_{WB}}$ on the basis of $E_{\mathrm{vol\ ave}}$, together with the average of the absolute values of the relative errors. Table VI shows that assessing $\mathrm{SAR_{WB}}$ on the basis of $E_{\mathrm{vol\ ave}}$ yields an average of the absolute values of the relative error of approximately 6% (with a maximum of -12%).
- $\mathrm{SAR_{1\ g}}$ and $\mathrm{SAR_{10\ g}}$ values show a rather complex and difficult-to-predict relation with reference to the

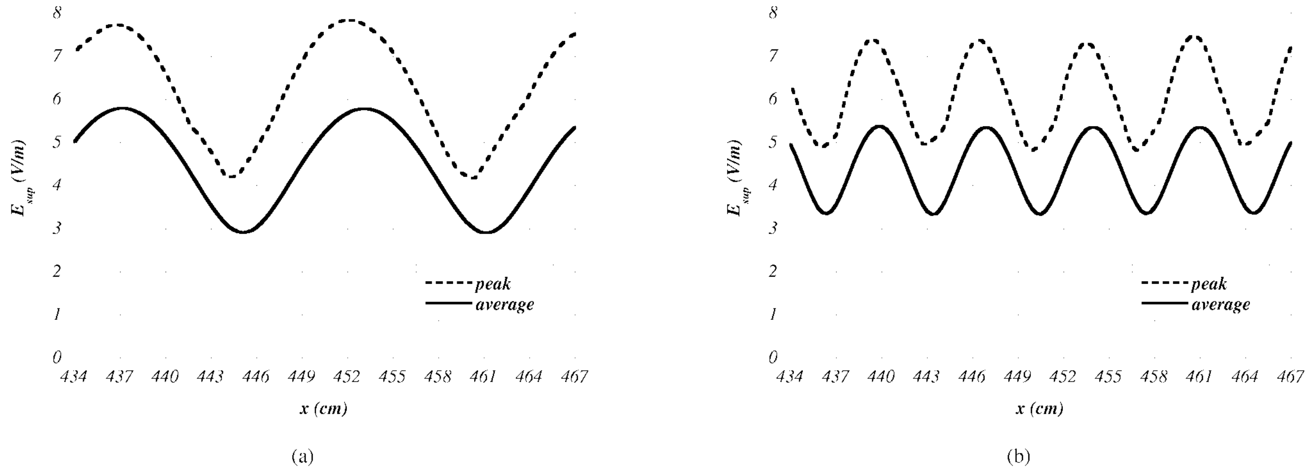

Fig. 4. Peak and average rms field values as a function of the position of the vertical surface inside the region where the subject will be placed for the "Front" case. (a) GSM antenna. (b) UMTS antenna.

TABLE III
COMPUTED SAR VALUES FOR ALL THE ANALYZED SCENARIOS: WHOLE-BODY AVERAGED SAR ($\mathrm{SAR_{WB}}$); PEAK 1-g AVERAGED SAR OVER THE BODY, EXCEPT HANDS, WRISTS, FEET, AND ANKLES ($\mathrm{SAR_{1\ g}}$); PEAK 10-g AVERAGED SAR OVER THE HEAD AND TRUNK ($\mathrm{SAR_{10\ g}}$); PEAK 10-g AVERAGED SAR OVER THE EXTREMITIES ($\mathrm{SAR_{10\ g\ extr}}$)—THE BODY PARTS WHERE PEAK VALUES OCCUR ARE ALSO REPORTED

Exposure Situation	SAR_{WB} (mW/kg)	SAR_{1g} (mW/kg)		SAR_{10g} (mW/kg)		$SAR_{10g\ extr}$ (mW/kg)	
		Val.	Pos.	Val.	Pos.	Val.	Pos.
Front GSM FS	0.409	11.76	face	4.75	face	8.45	hand
Front GSM Room	0.335	11.01	face	4.57	face	6.13	hand
Oblique GSM FS	0.309	4.92	arm	2.77	chest	6.31	foot
Oblique GSM Room	0.502	10.67	chest	6.18	chest	7.67	hand
Front UMTS FS	0.310	18.16	face	4.66	chin	4.89	elbow
Front UMTS Room	0.248	16.59	face	4.91	chin	4.86	arm
Oblique UMTS FS	0.245	5.47	face	2.97	chin	4.40	ankle
Oblique UMTS Room	0.159	4.90	arm	2.83	chin	2.84	ankle

TABLE IV
SQUARED RATIOS BETWEEN THE FIELD VALUES FOR EACH REALISTIC ENVIRONMENT AND THE VALUE COMPUTED IN THE RELATED FREE-SPACE CONDITION

Exposure Situation	$\left(\frac{E_{vol\ peak\ Room}}{E_{FS}}\right)^2$	$\left(\frac{E_{vol\ ave\ Room}}{E_{FS}}\right)^2$	$\left(\frac{E_{sup\ peak\ Room}}{E_{FS}}\right)^2$		$\left(\frac{E_{sup\ ave\ Room}}{E_{FS}}\right)^2$	
			min	max	min	max
Front GSM	2.279	0.786	0.643	2.279	0.313	1.244
Oblique GSM	6.260	1.425	2.508	6.260	0.885	2.226
Front UMTS	2.069	0.729	0.856	2.069	0.410	1.066
Oblique UMTS	4.994	0.653	2.268	4.994	0.546	0.799

exposure field. In order to get some insight into this relation, Fig. 5(a) and (b) reports, for each one of the considered environments, the relative error made assessing $\mathrm{SAR_{1\ g}}$ and $\mathrm{SAR_{10\ g}}$, respectively, on the basis of the different computed field values. The averages of the absolute values of the relative errors are also shown. From the analysis of Fig. 5, it can be stated that the use of the volume-averaged field value can lead to an underestimation of the local SAR values, up to 36%,

TABLE V
RATIOS BETWEEN SAR VALUES IN THE REALISTIC SCENARIO AND THE CORRESPONDING ONES IN FREE-SPACE CONDITIONS

Exposure Situation	$\frac{SAR_{WB\ Room}}{SAR_{WB\ FS}}$	$\frac{SAR_{1g\ Room}}{SAR_{1g\ FS}}$	$\frac{SAR_{10g\ Room}}{SAR_{10g\ FS}}$	$\frac{SAR_{10g\ extr\ Room}}{SAR_{10g\ extr\ FS}}$
Front GSM	0.820	0.936	0.962	0.725
Oblique GSM	1.626	2.169	2.231	1.216
Front UMTS	0.800	0.913	1.054	0.994
Oblique UMTS	0.649	0.896	0.953	0.645

TABLE VI
RELATIVE ERROR FOR EACH CONSIDERED SCENARIO AND AVERAGE OF THE ABSOLUTE VALUES OF THE RELATIVE ERRORS MADE ASSESSING $\mathrm{SAR_{WB}}$ ON THE BASIS OF $E_{\mathrm{vol\ ave}}$

Exposure Situation	Front GSM	Oblique GSM	Front UMTS	Oblique UMTS	Average
% error	-4.2 %	-12.4 %	-8.9 %	0.6 %	**6.5 %**

while, on the contrary, using the maximum volumetric value ($E_{\mathrm{sup\ peak\ max}}$) yields a relevant overestimation of local SAR (up to approximately four times). The studied situations suggest that the local SAR shows a good correlation with the maximum surface-averaged field value ($E_{\mathrm{sup\ ave\ max}}$) obtained varying the position of the vertical surface inside the volume occupied by the subject. In particular, the average of the absolute values of the relative errors is approximately 15% with a maximum of 33%. A possible approach, therefore, could consist of comparing this specific field value with the relevant reference level. Of course, this conclusion would require the study of an extended range of exposure conditions in order to be confirmed.

- $\mathrm{SAR_{10\ g\ extr}}$ does not show apparent relations with any of the computed field values. In any case, the SAR in the bodily extremities generally does not play an important role in compliance assessment and, therefore, can be neglected in the first instance.

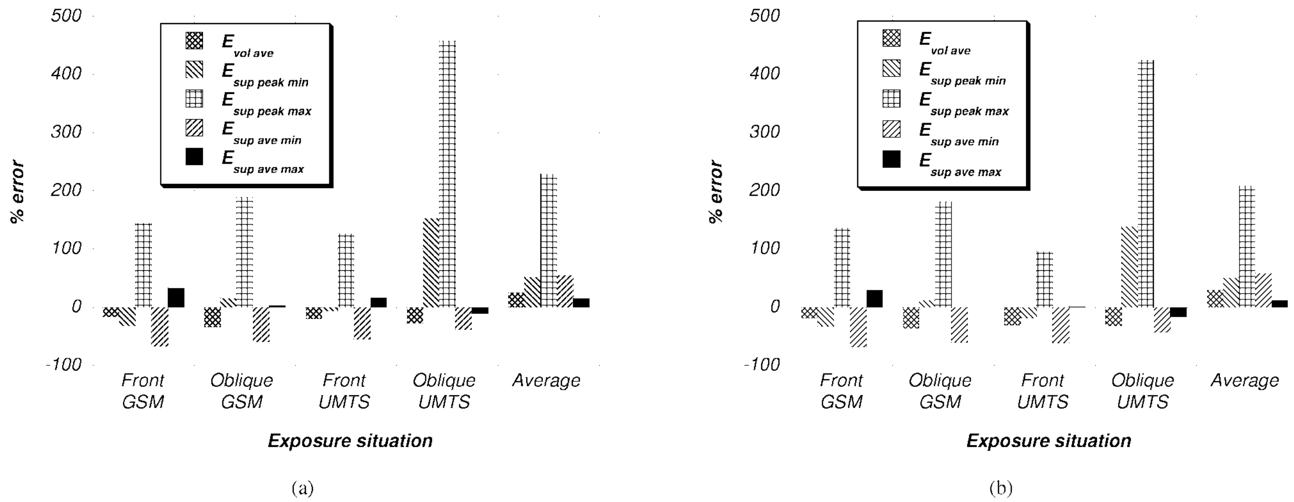

Fig. 5. Relative error made assessing: (a) $\mathrm{SAR}_{1\ \mathrm{g}}$ and (b) $\mathrm{SAR}_{10\ \mathrm{g}}$ on the basis of the different computed field values for each considered environment. The averages of the absolute values of the relative errors are also reported.

From the above discussion, it is possible to conclude that surface-averaged field values should be used with care because they are susceptible to large variations as the position of the surface is moved inside the volume occupied by the exposed body, and that the use of a volume-averaged value would be more consistent for $\mathrm{SAR}_{\mathrm{WB}}$ assessment. As concerns peak field values for local SAR compliance, the use of the volumetric peak seems to be too conservative, while a better approach could be the use of the maximum of the surface-averaged values.

In conclusion, a possible procedure to assess compliance could be to compute the average field values for different vertical surfaces and, from these, to derive a volume-averaged value to assess $\mathrm{SAR}_{\mathrm{WB}}$ compliance and the maximum surface-averaged value to assess $\mathrm{SAR}_{1\ \mathrm{g}}$ or $\mathrm{SAR}_{10\ \mathrm{g}}$ compliance.

Of course if such a procedure is applied in conjunction with measurements rather than numerical computations, it could become particularly time consuming, depending on the number of vertical surfaces considered and on the number of measurement points on each surface. On the other hand, the field distributions obtained, particularly in the UMTS frequency band (see Fig. 3), show a complex pattern with very quick spatial variations and, therefore, it can be expected that the use of only a few measurement points might lead to large errors in the average estimation. A convenient and accurate solution could be that of using an automated field-scanning system with data-logging capabilities in order to obtain a fine and quick measurement within a specific region. This region might be chosen as the one with potentially highest field values based on field predictions or on a coarse scan of the area of interest.

IV. Conclusions

Different realistic human-exposure situations inside a building for a GSM 900 and a UMTS base-station antenna installed in an urban environment have been studied using a UTD/FDTD technique. The different exposure conditions examined have been analyzed to highlight the problems related to compliance assessment procedures in complex exposure scenarios and to suggest some possible solutions.

A comparison of the numerical results obtained in the realistic environments with those computed in free space (neglecting the presence of the building walls) has evidenced that numerical compliance assessment should not be carried out considering simplified models because this could lead to a large underestimation of the real exposure. In particular, in the examined scenarios, underestimations up to a factor of two on SAR values have been evidenced, and they could be expected to be even higher for environments presenting more reflective and diffractive characteristics.

As concerns field nonuniformities and average field values, the obtained results have shown that surface-averaged fields should be used with care because of the large variations encountered as the position of the averaging surface is moved inside the volume occupied by the exposed subject. Moreover, it has been demonstrated that the whole-body averaged SAR is well related to the volume-averaged field value, while local SAR values show a more complex relation with the exposure field. In any case, local SAR compliance can be roughly assessed on the basis of the maximum surface-averaged value obtained varying the position of the averaging surface within the volume occupied by the exposed subject.

References

[1] *IEEE Standard for Safety Levels With Respect to Human Exposure to Radio Frequency Electromagnetic Fields, 3 kHz to 300 GHz*, IEEE Standard C95.1, 1999.

[2] "Evaluating compliance with FCC guidelines for human exposure to radiofrequency electromagnetic fields," FCC, Washington, DC, OET Bull. 65, Aug. 1997.

[3] "ICNIRP guidelines for limiting exposure to time-varying electric, magnetic, and electromagnetic fields (up to 300 GHz)," *Health Phys.*, vol. 74, no. 4, pp. 494–522, 1998.

[4] "Council recommendation on limits for exposure of the general public to electromagnetic fields: 0 Hz–300 GHz," Commission Eur. Communities, Brussels, Belgium, June 1998.

[5] *Basic Standard for the Calculation and Measurement of Electromagnetic Field Strength and SAR Related to Human Exposure From Radio Base Stations and Fixed Terminal Stations for Wireless Telecommunication Systems (110 MHz–40 GHz)*, CENELEC Standard EN 50383, 2002.

[6] *Guidance for Carrying Out a Base Radio Station Complying With Limits for Human Exposure to High Frequency Electromagnetic Fields*, Italian Electrotech. Committee Standard 211-10, 2002.

[7] Q. Balzano and A. Faraone, "Peak and average RF safety compliance levels near radio base station antennas—Prediction formulas and numerical validation," in *IEEE Int. Electromagnetic Compatibility Symp.*, Aug. 2001, pp. 780–785.

[8] Z. Altman, B. Begasse, C. Dale, A. Karwowski, J. Wiart, M. F. Wong, and L. Gattoufi, "Efficient models for base station antennas for human exposure assessment," *IEEE Trans. Electromagn. Compat.*, vol. 44, pp. 588–592, Nov. 2002.

[9] P. Bernardi, M. Cavagnaro, L. Cristoforetti, C. Malacarne, S. Pisa, E. Piuzzi, R. Pontalti, and A. Vaccari, "Modeling of BTS antennas: Dependence of the accuracy on FDTD mesh size and implementation criteria," in *Proc. 2nd Int. Biological Effects of Electromagnetic Fields Workshop*, vol. 1, P. Kostarakis, Ed., Rhodes, Greece, Oct. 2002, pp. 74–82.

[10] S. Blanch, J. Romeu, and A. Cardama, "Near field in the vicinity of wireless base-station antennas: An exposure compliance approach," *IEEE Trans. Antennas Propagat.*, vol. 50, pp. 685–692, May 2002.

[11] G. Lazzi, O. P. Gandhi, and D. Sullivan, "Fast and efficient FDTD simulations of personal wireless devices for SAR compliance testing and antenna design," in *IEEE AP-S Int. Symp.*, July 2000, pp. 1088–1091.

[12] E. Nicolas, D. Lautru, F. Jacquin, M. F. Wong, and J. Wiart, "Specific absorption rate assessments based on a selective isotropic measuring system for electromagnetic fields," *IEEE Trans. Instrum. Meas.*, vol. 50, pp. 397–401, Apr. 2001.

[13] J. Cooper, B. Marx, J. Buhl, and V. Hombach, "Determination of safety distance limits for a human near a cellular base station antenna, adopting the IEEE standard or ICNIRP guidelines," *Bioelectromagnetics*, vol. 23, pp. 429–443, 2002.

[14] P. Bernardi, M. Cavagnaro, S. Pisa, and E. Piuzzi, "Human exposure in the vicinity of radio base station antennas," in *Proc. Eur. Electomagnetic Compaibility Symp.*, Sept. 2000, pp. 187–192.

[15] ——, "Human exposure to cellular base station antennas in urban environment," *IEEE Trans. Microwave Theory Tech.*, vol. 48, pp. 1996–2002, Nov. 2000.

[16] M. Alaydrus, A. Bitz, J. Streckert, and V. Hansen, "Combination of the hybrid$^{(2)}$—Method and the FDTD for safety assessment of human for base station antennas mounted in real environments," presented at the *XXVIIth General Assembly of Int. Union of Radio Science*, Aug. 2002, Paper 872.

[17] A. Taflove, *Computational Electrodynamics: The Finite-Difference Time-Domain Method*. Norwood, MA: Artech House, 1995.

[18] K. S. Kunz and R. J. Luebbers, *The Finite Difference Time Domain Method for Electromagnetics*. Boca Raton, FL: CRC, 1993.

[19] A. Taflove, *Advances in Computational Electrodynamics: The Finite-Difference Time-Domain Method*. Norwood, MA: Artech House, 1998.

[20] P. Bernardi, R. Cicchetti, and O. Testa, "A three-dimensional UTD heuristic diffraction coefficient for complex penetrable wedges," *IEEE Trans. Antennas Propagat.*, vol. 50, pp. 217–224, Feb. 2002.

[21] ——, "An accurate UTD model for the analysis of complex indoor radio environments in microwave WLAN systems," *IEEE Trans. Antennas Propagat.*, to be published.

[22] ——, "An electromagnetic characterization of indoor radio environment in microwave WLAN systems," in *IEEE MTT-S Int. Microwave Symp. Dig.*, May 2001, pp. 1101–1104.

[23] P. Bernardi, M. Cavagnaro, P. D'Atanasio, E. Di Palma, S. Pisa, and E. Piuzzi, "FDTD, multiple-region/FDTD, ray-tracing/FDTD: A comparison on their applicability for human exposure evaluation," *Int. J. Numer. Modeling*, vol. 15, no. 5–6, pp. 579–593, Sept.–Dec. 2002.

[24] S. D. Gedney, "An anisotropic perfectly matched layer-absorbing medium for the truncation of FDTD lattices," *IEEE Trans. Antennas Propagat.*, vol. 44, pp. 1630–1639, Dec. 1996.

[25] "Digital cellular telecommunication system, radio transmission and reception," ETSI, Sophia Antipolis, France, Tech. Specification GSM 05.05, 1996.

[26] "UMTS; UTRA (BS) FDD; Radio Transmission and Reception," ETSI, Sophia Antipolis, France, Tech. Specification TS 125 104, 2000.

[27] J. Burke and A. Poggio, "Numerical electromagnetics code (NEC)—Method of moments," Lawrence Livermore Nat. Lab., Livermore, CA, Rep. UCID-18 834, 1981.

[28] C. Yang, B. Wu, and C. Ko, "A ray-tracing method for modeling indoor wave propagation and penetration," *IEEE Trans. Antennas Propagat.*, vol. AP-46, pp. 907–919, June 1998.

[29] P. A. Mason, J. M. Ziriax, W. D. Hurt, T. J. Walters, K. L. Ryan, D. A. Nelson, K. I. Smith, and J. A. D'Andrea, "Recent advancements in dosimetry measurements and modeling," in *Radio Frequency Radiation Dosimetry*, B. J. Klauenberg and D. Miklavcic, Eds. Norwell, MA: Kluwer, 2000, pp. 141–155.

[30] O. P. Gandhi, Y. Gu, J. Y. Chen, and H. I. Bassen, "Specific absorption rates and induced current distribution in an anatomically based human model for plane-wave," *Health Phys.*, vol. 63, pp. 281–290, 1992.

[31] P. Bernardi, M. Cavagnaro, and S. Pisa, "Assessment of the potential risk for humans exposed to millimeter-wave wireless LANs: The power absorbed in the eye," *Wireless Networks*, vol. 3, pp. 511–517, 1997.

[32] S. Gabriel, R. W. Lau, and C. Gabriel, "The dielectric properties of biological tissues: III. Parametric models for the dielectric spectrum of tissues," *Phys. Med. Biol.*, vol. 41, pp. 2271–2293, 1996.

[33] C. Gabriel, "Compilation of the dielectric properties of body tissues at RF and microwave frequencies," Brooks Air Force Base, Brooks AFB, TX, Tech. Rep. AL/OE-TR-1996-0037, 1996.

[34] P. Bernardi, M. Cavagnaro, R. Cicchetti, S. Pisa, E. Piuzzi, and O. Testa, "A UTD/FDTD model to evaluate human exposure to base-station antennas in realistic urban environments," in *IEEE MTT-S Int. Microwave Symp. Dig.*, June 2003, pp. 403–406.

Paolo Bernardi (M'66–SM'73–F'93–LF'01) was born in Civitavecchia, Italy, in 1936. He received the Electrical Engineering and Libera Docenza degrees from the University of Rome, Rome, Italy, in 1960 and 1968, respectively.

Since 1961, he has been with the Department of Electronics, University of Rome "La Sapienza," Rome, Italy, where he became a Full Professor in 1976 and served as Head of the Department from 1982 to 1988. He has authored over 180 scientific papers and numerous invited presentations at international workshops and conferences. His research has dealt with the propagation of EM waves in ferrites, microwave components, biological effects of EM waves, and EM compatibility. He is currently on the Editorial Board for *Microwave and Optical Technology Letters*. He was an Associate Editor for the *URSI Radio Science Bulletin*. He was the Guest Editor of special issues on "Nonionizing Electromagnetic Radiation" of *Alta Frequenza* (March 1980) and "Exposure Hazards and Health Protection in Personal Communication Services" of *Wireless Networks* (December 1997).

Dr. Bernardi is a member of the Bioelectromagnetics Society (BEMS), European Bioelectromagnetics Association (EBEA), and "Socio Fedele" of the Italian Electrical and Electronic Society (AEI). From 1979 to 1980, he was the chairman of the IEEE Middle and South Italy Section. He was chairman of the International Union of Radio Science (URSI) Commission K on Electromagnetics in Biology and Medicine (1993–1996), vice-chairman of the European Community COST Project 244 on Biomedical Effects of Electromagnetic Radiation (1993–1997), and project coordinator of the European Community Project CEPHOS (1998–2000), which was devoted to EM dosimetry and compliance with standards of mobile cellular phones. He is currently the scientific coordinator of the Italian National Project (2001–2004) devoted to the protection of people and environment from the EM emissions. He was an Editorial Board member for the IEEE TRANSACTIONS ON MICROWAVE THEORY AND TECHNIQUES. He was the recipient of the 1984 IEEE Centennial Medal.

Marta Cavagnaro (M'01) was born in Rome, Italy, in 1966. She received the Electronic Engineering (*cum laude*) and Ph.D. degrees from the University of Rome "La Sapienza," Rome, Italy, in 1993 and 1997, respectively.

She is currently with the Department of Electronic Engineering, University of Rome "La Sapienza," as an Assistant Professor. Her current research interests are dosimetric aspects of the interaction between EM fields and biological systems and numerical techniques.

Dr. Cavagnaro was the recipient of the 1996 International Union of Radio Science (URSI) Young Scientist Award.

Renato Cicchetti (S'83–M'83–SM'01) was born in Rieti, Italy, in May 1957. He received the Laurea degree (*summa cum laude*) in electronic engineering from the University of Rome "La Sapienza," Rome, Italy, in 1983.

From 1983 to 1986, he was an Antenna Designer with Selenia Spazio S.p.A. (now Alenia Aerospazio S.p.A.), Rome, Italy, where he was involved in studies on theoretical and practical aspects of antennas for space application and scattering problems. From 1986 to 1994, he was a Researcher, and from 1994 to 1998, he was an Assistant Professor with the Department of Electronic Engineering, University of Rome "La Sapienza," where he is currently an Associate Professor. In 1998 and in 2002, he was a Visiting Professor with the Motorola Florida Corporate Electromagnetics Research Laboratory, Fort Lauderdale, FL, where he was involved with antennas for cellular and wireless communications. He is currently the coordinator of the activity "electromagnetic compatibility/electromagnetic interference (EMC/EMI) characterization of an airport environment in the presence of complex electromagnetic sources" of the Italian national project (2001–2004) funded by the Italian Ministry for Education, University, and Research, and is devoted to the protection of people and environment from EM emissions. He also serves as a reviewer of several scientific journals. His current research interests include electromagnetic-field theory, asymptotic techniques, electromagnetic compatibility, wireless communications, microwave and millimeter-wave integrated circuits, and antennas. He is listed in Marquis's *Who's Who in the World* and *Who's Who in Science and Engineering*.

Dr. Cicchetti is a member of the Italian Electrical and Electronic Society (AEI).

Stefano Pisa (M'91) was born in Rome, Italy, in 1957. He received the Electronic Engineering and Ph.D. degrees from the University of Rome "La Sapienza," Rome, Italy, in 1985 and 1988, respectively.

In 1989, he joined the Department of Electronic Engineering, University "La Sapienza," as a Researcher. Since 2001, he has been an Associate Professor with the same university. His research interests are the interaction between EM fields and biological systems, therapeutic and diagnostic applications of EM fields, and the modeling and design of microwave circuits.

Dr. Pisa was the editor of the Disk of Complete References 1993–1995 for the Commission K (Electromagnetics in Biology and Medicine) of the International Union of Radio Science (URSI), published at the 25th URSI General Assembly. From 1995 to 1996, he was the coordinator of a "working package" on "Electromagnetic Environment Impact and Safety Issues" of the Italian project on "Wide Band Wireless Local Area Networks—WWLAN" of the Italian Research Council (CNR). From 1995 to 1999, he was a member of the Joint Working Group (JWG) 15 on "Measurement Techniques and Procedures for High-Frequency EM Fields With Regard to Human Exposure in the Frequency Range 10 kHz–300 GHz" created by International Electrotechnical Commission (IEC). From 1997 to 1999, he was the coordinator of the working package "Survey on Existing Dosimetric Work and Development of a Database" in the framework of the European project "Cellular Phones Standard" (CEPHOS). From 1995 to 2002, he was secretary of the IEEE Microwave Theory and Techniques Society (MTT-S)/Antennas and Propagation Society (AP-S) Central and South Italy Section Joint Chapter. He is currently the coordinator of the activity "Development and Optimization of Dedicated Software for the Evaluation of SAR in Subjects Exposed to Mobile Telecommunication Systems" of the Italian National Project (2001–2004) funded by the Italian Ministry for Education, University, and Research, and devoted to the protection of people and environment from EM emissions.

Emanuele Piuzzi was born in Galatina, Lecce, Italy, in 1972. He received the Electronic Engineering (*cum laude*) and Ph.D. degrees from the University of Rome "La Sapienza," Rome, Italy, in 1997 and 2001, respectively.

He is currently with the Department of Electronic Engineering, University of Rome "La Sapienza." His main research interests are related to the study of the interaction between EM fields radiated by mobile communication systems and exposed subjects and of therapeutic applications of EM fields (microwave tissue ablation and hyperthermic cancer treatment). He is currently studying smart antennas for cellular base stations.

Dr. Piuzzi was the recipient of one of the 1999 International Union of Radio Science (URSI) Young Scientist Awards. He is currently the recipient of a University of Rome "La Sapienza," research fellowship.

Orlandino Testa was born in Minturno, Italy, in August 1972. He received the Electronic Engineering degree (*cum laude*) and the Ph.D. degree from the University of Rome "La Sapienza," Rome, Italy, in 1997 and 2003, respectively.

Since 2001 he has been a High School Teacher with the ITIS "G. Armellini" Institute of Rome, Rome, Italy, where he is involved in teaching electronics and telecommunications. He also currently collaborates with the Department of Electronic Engineering, University of Rome "La Sapienza." He currently studies high-frequency models for the analysis of complex indoor radio environments with particular attention to EMC/EMI problems. His main research interests are propagation and radiation of electromagnetic fields, electromagnetic compatibility, microwave and millimeter-wave integrated circuits, and antennas.